VOL. 11, NO. 19, OCTOBER 2016 ISSN 1819-6608
ARPN Journal of Engineering and Applied Sciences

www.arpnjournals.com

TRANSFORMATION AND INTERFERENCE OF THE LASER RADIATION IN COMPOSITE CRYSTAL OPTICAL SYSTEMS

Abilhan Umbetovich Umbetov, Makhabbat Zhaksylykovna Umbetova, Gabit Mukhitovich Abildayev, Saule Svyazkhanovna Baizakova, Samal Arynovna Zhamalova, Arailym Boranbayevna Konussova and Kalamkul Kapenovna Dosmagulova
Arkalyk State Pedagogical Institute after I. Altynsarin, Auelbekova Street, Arkalyk, Republic of Kazakhstan
E-Mail: Umbetov.a@mail.ru

ABSTRACT

Currently, the use of crystal optical systems in the scientific and technological development has increased significantly. With their help it is possible to solve the control tasks of the amplitude, frequency, phase and polarization of the laser radiation and scanning by an optical beam in space. In addition, crystal optical systems are used for spatial encoding; creating controlled spatial filters in polarization interferometers, allowing investigating the quality of processing of optical parts, geometric parameters of the laser beams, the degree of coherence of the laser radiation to a high precision. When the laser radiation is placed at the output of crystal optical systems, there appear the interference patterns, which are applied for various purposes in laser measuring devices. The construction of circuit schemes and laser devices should continually be improved to enhance their capacity, accuracy, sensitivity, reliability and service life. Providing a solution for these problems is possible upon condition of new ideas that have emerged in crystal optics and laser technology.

Keywords: interference, laser, radial vector composite system, path difference, dispersion vector, optical field.

1. INTRODUCTION

The investigation of composite crystal optical systems (CCOS) of anisotropic crystals is of interest for the construction of laser measuring devices. This raises the problem of the development of methods of calculation for such systems, which would describe more accurately their properties for the transmission and interference of electromagnetic waves (laser radiation) [1], [2]. This paper studies the distribution of the laser radiation through composite crystal optical systems made from uniaxial Iceland spar crystals. The research is based on newly developed techniques and examines the interference mode of the polarized laser radiation generated in the CCOS [3].

As shown in Figure-1, the CCOS consists of plano-concave (I) and plano-convex (II) uniaxial crystal lenses with different directions of optical axes in I and II, specified unit vectors $\vec{a}_1$ (1,0,0) и $\vec{a}_2$ (0, $\sin\psi$, $\cos\psi$), where the ψ-angle is between $\vec{a}_2$ and the z axis, respectively.

A well-known covariant calculating method [4], [5] of the laser radiation in anisotropic media leads to composite general expressions, and its use for CCOSs is difficult. In general, the problem is not amenable to a rigorous analytical solution, where the main difficulty is the need to take into account the non-parallelism of the wave vector $\kappa = 2\pi / \lambda$ describing the transfer of the wave phase, and the radial vector $\vec{S} = [\vec{E}\vec{H}]$, describing the transfer of the wave energy (λ-the length of the wave, $\vec{E}, \vec{H}$ - the intensity vectors of the electric and magnetic fields).

This paper solves the problem of extending the ordinary (0) and extraordinary (e) waves in an anisotropic dielectric medium with regard to the boundary conditions for the CCOS with the simplest and at the same time sufficiently general methods of geometrical optics in paraxial approximation, i.e. in supposing an infinitely narrow parallel beam, falling on different points of the input face of the anisotropic medium [6]. This calculating method of the laser radiation in anisotropic media allows to identify all the basic properties of the studied CCOS and to compare the results of theoretical calculations with experimental data. It also allows to describe in detail the interference mode of the laser radiation and to make assumptions of its use in laser polarized interferometers [7].

The calculations of the path of beams in the CCOS, known in the literature [8], are limited to the case of normal incidence of light in the input face of the system and held for each individual system separately. Shafranovsky and Fedorov studied the method of calculation of the beams' path in refracting prisms of variable doubling angle [9]. The current paper considers the calculation of the path of electromagnetic waves in anisotropic uniaxial and biaxial crystals, the laws of reflection and refraction at the interface of two anisotropic media [10].

Therefore, the purpose of this research is to develop efficient techniques for calculation (transformation) of the path of laser radiation, to study the interference patterns when transmitting through the crystal optical system and the dispersion properties of the CCOS. Research objectives are as follows:

- Conducting a comprehensive study of the crystal optical system, the properties of transformation of the laser radiation when transmitting through the CCOS;
- Investigating the conditions for the occurrence of interference patterns at the output of the CCOS and their possible use in a variety of laser measuring devices;
- Studying the dispersion properties of the CCOS.

2. METHODS

This research studies the theory of distribution of electromagnetic waves (laser radiation) in anisotropic crystals, the laws of reflection and refraction at the interfaces of media [11]. The covariant method by F.I. Fedorov for calculating the distribution of electromagnetic waves in anisotropic media is known. However, a rigorous calculation of the beams' path in crystal optical systems consisting of several anisotropic crystals results in cumbersome expressions, not suitable for engineering calculations and for investigating the general optical and interference properties of crystal optical systems. An effective calculating technique of the path of electromagnetic waves (laser radiation) in composite crystal optical systems and a description of the conditions for the occurrence of interference patterns at the output of the CCOS are required [12], [13].

This paper proposes a simple and fairly common technique of geometrical optics in paraxial approximation. For example, suppose that the narrow parallel beam of light with a circular polarization falls on the left face of the CCOS (on the XY plane) at an arbitrary point M (Figure 2) along the Z-axis. If we denote the coordinates of the point M on the XY plane: dcosφ, dsinφ, 0), where φ is the angle between the X-axis and the radius - vector d, drawn from the origin z=0 to the point M, then the assumption that d,<<R, where R is the radius of curvature of the spherical CCOS interface and the value $(\frac{d}{R})^2$ will be negligible.

3. RESULTS AND DISCUSSIONS

The ways of transformation of the laser radiation through a composite crystal optical system are diverse, formed with the help of interference patterns. At the output of the CCOS, there are four beams with the same polarization states, but orthogonal between the pairs. However, a different distribution of the incident beam energy in the CCOS among four outgoing beams keeps the number of ongoing interference patterns under certain experimental conditions.

An exhaustive answer can be obtained by solving the Fresnel task to find the amplitudes of all the waves on three interfaces (Figure-1).

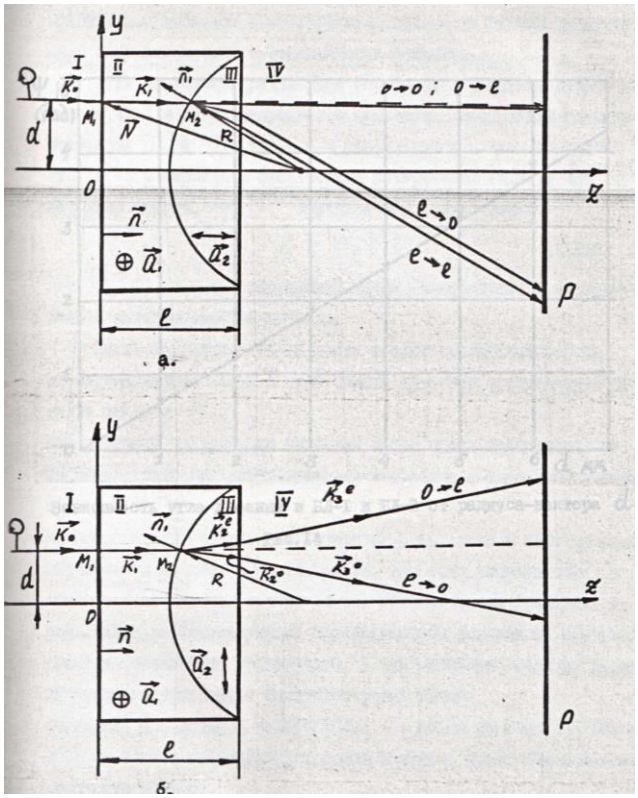

Figure-1. Composite crystal optical systems: A - CCOS-1 type, B - CCOS-2 type.

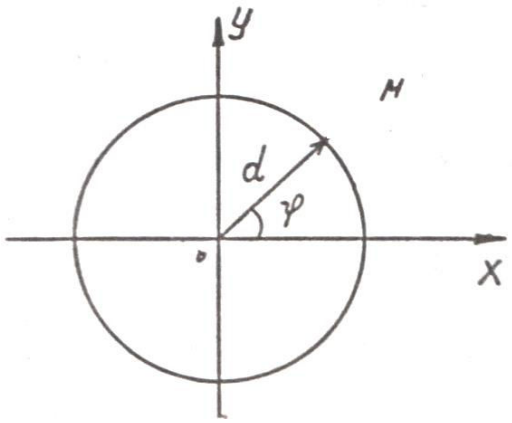

Figure-2. Location of the point M and the parameters in the XY plane.

This problem cannot be completely solved by analytical methods. Nevertheless, sufficient information about the amplitudes of beams can be obtained from the following simple reasoning.

A flat (monochromatic) electromagnetic wave at the input face of the CCOS-1 is divided into two waves with orthogonal polarizations. The vibration directions of $\overrightarrow{E_0}$ и $\overrightarrow{Д_0}$ and $\overrightarrow{E_0}$ и $\overrightarrow{Д_0}$ vectors for the o(ordinary) wave coincide and are perpendicular to the main plane of the crystal. The unit vector of the electric vector (o) of the wave in the field I of the CCOS-1 can be written as follows:

$$\overrightarrow{e_0^{(1)}} = \frac{[\overrightarrow{\kappa_1}\,\overrightarrow{a_1}]}{|[\overrightarrow{\kappa_1}\,\overrightarrow{a_1}]|} = \frac{[\overrightarrow{\kappa_1}\,\overrightarrow{a_1}]}{\sqrt{1-(\overrightarrow{\kappa_1}\,\overrightarrow{a_1})^2}} \quad (1)$$

the vibration directions of $\overrightarrow{E_0}$ и $\overrightarrow{Д_0}$ and $\overrightarrow{E_0}$ и $\overrightarrow{Д_0}$ vectors for the e(extraordinary) wave lie in the main plane and in general do not coincide. Given that the $\overrightarrow{Д_0}$ vector is perpendicular to the direction of the wave distribution and is related to the $\overrightarrow{E}$ vector by the ratio $\overrightarrow{Д_e} = \varepsilon_o\varepsilon\overrightarrow{E}$,, the unit vector of the electric vector can be written as follows:

$$\overrightarrow{e_e^{(1)}} = \frac{\varepsilon_1^{-1}[\overrightarrow{\kappa_1}[\overrightarrow{\kappa_1}\overrightarrow{a_1}]]}{|\varepsilon_1^{-1}[\overrightarrow{\kappa_1}[\overrightarrow{\kappa_1}\overrightarrow{a_1}]]|} = \frac{\left[\overrightarrow{S_1}[\overrightarrow{\kappa_1}\overrightarrow{a_1}]\right]}{\left|\left[\overrightarrow{S_1}[\overrightarrow{\kappa_1}\overrightarrow{a_1}]\right]\right|}, \quad (2)$$

where ε^{-1} is the inverse matrix of dielectric permeability of the crystal, $\overrightarrow{S_1}$ – the radial vector. For the field II of the CCOS-1, the vibration direction of the electric vector of (o) and (e) waves will be as follows:

$$\overrightarrow{e_2^{(1)}} = \frac{[\overrightarrow{\kappa_2}\,\overrightarrow{a_2}]}{\sqrt{1-(\overrightarrow{\kappa_2}\,\overrightarrow{a_2})^2}}\ \overrightarrow{e_e^{(2)}} = \frac{\varepsilon_2^{-1}[\overrightarrow{\kappa_2}[\overrightarrow{\kappa_2}\overrightarrow{a_2}]]}{|\varepsilon_2^{-1}[\overrightarrow{\kappa_2}[\overrightarrow{\kappa_2}\overrightarrow{a_2}]]|} = \frac{\left[\overrightarrow{S_2}[\overrightarrow{\kappa_2}\overrightarrow{a_2}]\right]}{\left|\left[\overrightarrow{S_2}[\overrightarrow{\kappa_2}\overrightarrow{a_2}]\right]\right|} \quad (3)$$

where ε_2^{-1} – the inverse matrix of dielectric permeability in the field II of the CCOS-1 and $\overrightarrow{S_2}$ - the radial vector.
Suppose that the wave, falling on the input face of the CCOS-1, has a circular polarization. Then (o) and (e) waves in the field I of the CCOS-1 will have an equal amplitude:

$$\overrightarrow{E_0^{(1)}} = A\overrightarrow{e_0^{(1)}};\ \overrightarrow{E_e^{(1)}} = A\overrightarrow{e_2^{(1)}} \quad (4)$$

On a spherical surface each of these waves are split again into o- and e- waves. The amplitudes of these waves will depend on the relative orientation of optical axes in the field I and II of the CCOS-1, and if we neglect the reflected waves, the electric vectors can be written as a projection of the electric vector in the field I of the CCOS-1 in the vibration direction in the field II of the CCOS-1:

$$\overrightarrow{E_0^{(2)}} = A\overrightarrow{e^{(1)}}(\overrightarrow{e^{(1)}}\overrightarrow{e_0^{(2)}});\ \overrightarrow{E_e^{(2)}} = A\overrightarrow{e^{(1)}}(\overrightarrow{e^{(1)}}\overrightarrow{e_e^{(2)}}), \quad (5)$$

where $\overrightarrow{e^{(1)}}$ – the unit vector of the electric vector of the wave falling on the spherical surface.

The wave with the polarization of the o- wave in the field I of the CCOS-1 on the spherical surface will be split into o- and e- waves:

$$\overrightarrow{E_{00}^{(2)}} = A\overrightarrow{e_0^{(1)}}\left(\overrightarrow{e_0^{(1)}}\overrightarrow{e_0^{(2)}}\right);\ \overrightarrow{E_{0e}^{(2)}} = A\overrightarrow{e_0^{(1)}}(\overrightarrow{e_0^{(1)}}\overrightarrow{e_e^{(2)}}) \quad (6)$$

The transmission coefficient of the o- wave by intensity is determined by (4) and (6) ratio:

$$d_{00} = \frac{\left|\overrightarrow{E_{00}^{(2)}}\right|^2}{\left|\overrightarrow{E_0^{(1)}}\right|^2} = \frac{\left|A\overrightarrow{e_0^{(1)}}\right|^2\left|\overrightarrow{e_0^{(1)}}\overrightarrow{e_0^{(2)}}\right|^2}{\left|A\overrightarrow{e_0^{(1)}}\right|^2} = \frac{([\overrightarrow{\kappa_1}\overrightarrow{a_1}][\overrightarrow{\kappa_2}\,\overrightarrow{a_2}])^2}{(1-(\overrightarrow{\kappa_1}\overrightarrow{a_1})^2)(1-(\overrightarrow{\kappa_2}\,\overrightarrow{a_2})^2)} \quad (7)$$

As far as the o- wave is not refracted at the interface of the lens, then $\overrightarrow{\kappa_0^{(1)}} = \overrightarrow{\kappa_0^{(2)}}$ and for the CCOS-1 with mutually perpendicular optical axes in the fields I and II we have:

$$d_{00} = \frac{(\overrightarrow{\kappa_1}\overrightarrow{a_1})^2(\overrightarrow{\kappa_2}\,\overrightarrow{a_2})^2}{(1-(\overrightarrow{\kappa_1}\overrightarrow{a_1})^2)(1-(\overrightarrow{\kappa_2}\,\overrightarrow{a_2})^2)} \quad (8)$$

Neglecting the reflection losses in the calculation of the coefficient of transformation of the (o) wave into the (e) wave, we have:

$$d_{0e}=1 - d_{00} = \frac{1-(\overrightarrow{\kappa_1}\overrightarrow{a_1})^2(\overrightarrow{\kappa_2}\,\overrightarrow{a_2})^2}{(1-(\overrightarrow{\kappa_1}\overrightarrow{a_1})^2)(1-(\overrightarrow{\kappa_2}\,\overrightarrow{a_2})^2)} \quad (9)$$

In the field I of the CCOS-1 the wave with polarization of the e - wave on the spherical surface of the interface will be split into o - and e - waves:

$$\overrightarrow{E_{e0}} = A\overrightarrow{e_e^{(1)}}\left(\overrightarrow{e_e^{(1)}}\overrightarrow{e_0^{(2)}}\right);\ \overrightarrow{E_{ee}^{(2)}} = A\overrightarrow{e_e^{(1)}}(\overrightarrow{e_e^{(1)}}\overrightarrow{e_e^{(2)}}) \quad (10)$$

Neglecting the reflection losses, the transmission coefficient of the e- wave by intensity can be written as:

$$d_{ee} = \frac{\left(\left[\overrightarrow{S_1}[\overrightarrow{\kappa_1}\overrightarrow{a_1}]\right]\left[\overrightarrow{S_2}[\overrightarrow{\kappa_2}\overrightarrow{a_2}]\right]\right)^2}{\left|\left[\overrightarrow{S_1}[\overrightarrow{\kappa_1}\overrightarrow{a_1}]\right]\left[\overrightarrow{S_2}[\overrightarrow{\kappa_2}\overrightarrow{a_2}]\right]\right|^2} \quad (11)$$

If to consider the correlation (9) and (10), which can be given within the accuracy of δ^2as:

$$(\vec{K}\,\vec{S}) = 1\,(\vec{S}\,\vec{A}) = (\vec{K}\,\vec{A})(1+\delta-\delta(\vec{K}\,\vec{A})^2) \quad (12)$$

the equation (11) will take the form:

$$d_{ee} = \frac{(\overrightarrow{\kappa_1}\overrightarrow{a_1})^2(\overrightarrow{\kappa_2}\,\overrightarrow{a_2})^2}{(1-(\overrightarrow{\kappa_1}\overrightarrow{a_1})^2)(1-(\overrightarrow{\kappa_2}\,\overrightarrow{a_2})^2)} \quad (13)$$

Without regard to reflection, the coefficient of transformation of the e- wave into the o- wave by intensity is equal to:

$$d_{e0} = 1 - \frac{(\overrightarrow{\kappa_1}\overrightarrow{a_1})^2(\overrightarrow{\kappa_2}\,\overrightarrow{a_2})^2}{(1-(\overrightarrow{\kappa_1}\overrightarrow{a_1})^2)(1-(\overrightarrow{\kappa_2}\,\overrightarrow{a_2})^2)} \quad (14)$$

At the output of the CCOS-1 there is no mutual transformation of vibration modes (o and e). Therefore, within the accuracy of reflection losses, the formula (8), (9), (13) and (14) define the intensity of beams at the output of the CCOS-1.

The equation (8) shows that if the radiation is falling in the plane of optical axis, then $(\overrightarrow{\kappa_1}\overrightarrow{a_1})^2 = 1 - (\overrightarrow{\kappa_1}\overrightarrow{a_1})^2$, $(\overrightarrow{\kappa_1}\overrightarrow{a_2})^2 = 1 - (\overrightarrow{\kappa_1}\overrightarrow{a_2})^2$ and the coefficient of transmission of the o- wave is $d_{oo} = I$. In other words, the o- wave does not change its polarization when transmitting the interface in the CCOS-1 from the field I to the field II.

If the radiation is falling normally towards the optical axis plane, then $\overrightarrow{\kappa_1}\overrightarrow{a_1} = 0$, $\overrightarrow{\kappa_1}\overrightarrow{a_2} = 0$ иand the coefficient of transformation is $d_{e0} = I$. Thus, the o- wave

is transforming entirely into the e- wave when transmitting through the spherical surface. If the radiation is falling in the plane which is perpendicular to the plane of optical axes of the CCOS-1, and contains one of them, the transformation coefficient is set to unity at any angle of incidence of the wave on the input face.

With the $\overrightarrow{\kappa_2}$ vector being presented in the form $\overrightarrow{\kappa_2} = \overrightarrow{\kappa_1} + \delta\overrightarrow{K_2^{(1)}}$, the expression (13) within the accuracy of δ^2can be written as follows:

$$d_{ee} = \frac{(\overrightarrow{\kappa_1 a_1})^2(\overrightarrow{\kappa_2 a_2})^2}{(1-(\overrightarrow{\kappa_1 a_1})^2)(1-(\overrightarrow{\kappa_2 a_2})^2)}\left[1 + 2\delta\frac{\left(\overrightarrow{\kappa_2^{(1)}a_1}\right)}{(\overrightarrow{\kappa_1 a_1})} + 2\delta\frac{\left(\overrightarrow{\kappa_2^{(1)}a_2}\right)(\overrightarrow{\kappa_1 a_2})}{1-(\overrightarrow{\kappa_1 a_2})^2}\right] \quad (15)$$

If the wave vector of the incident radiation lies in the plane of optical axes, then

$$d_{ee} = 1 + \frac{2\delta}{(\overrightarrow{\kappa_1 a_1})}\left[\left(\overrightarrow{\kappa_2^{(1)}a_1}\right)(\overrightarrow{\kappa_1 a_1}) + \left(\overrightarrow{\kappa_2^{(1)}a_2}\right)(\overrightarrow{\kappa_1 a_2})\right] \quad (16)$$

Given that $\overrightarrow{\kappa_2^{(1)}}$ lies in the plane containing $\overrightarrow{n_1}$ and и $\overrightarrow{K_1}$ $\left(\overrightarrow{K_2^{(1)}} = \alpha_2^{(1)}\overrightarrow{n_1} + +\beta_2^{(1)}\overrightarrow{K_1}\right)$, it can be concluded that the e- wave is not converted at the spherical interface of the CCOS-1 and remains the e- wave for the field II of the CCOS ($d_{ee} = I$), provided that the incidence of the beam is in the plane containing the optical axes, and this plane is parallel to the input and output faces ($\overrightarrow{K_2^{(1)}}$lies in the plane of optical axes), the e- wave at the interface is completely transformed into the o- wave, if the light beam is normally falling towards the plane of optical axes containing one of the axes.

In the lens of the CCOS-2 type, the plane of optical axes is parallel to the input and output faces, and therefore, at low angles of incidence on the input face, at the output of the CCOS-2, the basic intensity will have the waves transformed at the interface from the o- wave into the e- wave, from the e- wave into in the o- wave. When the radiation is falling in the plane perpendicular to the input face which contains one of the optical axes, only these two basic waves (o and e) will remain at the output of the CCOS-1 at any angle of incidence.

Let us estimate the intensity of the waves formed at the output of the CCOS-1. If the wave vector of the wave falling on the CCOS-1 is represented as:

$$\overrightarrow{K_0} = (\sin\alpha; 0; \cos\alpha) \quad (17)$$

then the wave vectors (o) and (e) of the waves in the field I in the CCOS-1 are:

$$\overrightarrow{K_1^0} = \left\{\frac{\sin\alpha}{n_0}; 0; \sqrt{1 - \frac{\sin^2\alpha}{n_0}}\right\} \quad (18)$$

$$\overrightarrow{K_1^e} = \{\sin\alpha_1^e; 0; \cos\alpha_1^e\} \quad (19)$$

With regard to the expression (4), from (19) we have:

$$\overrightarrow{K_1^e} = \left\{\frac{n_e\sin\alpha}{\sqrt{n_0^2n_e^2-(n_0^2-n_e^2)\sin^2\alpha}}; 0; \frac{n_0\sqrt{n_e^2-\sin^2\alpha}}{\sqrt{n_0^2n_e^2-(n_0^2-n_e^2)\sin^2\alpha}}; \right\} \quad (20)$$

In the field II of the CCOS-1 for the wave having the polarization of the e- wave on both sides of the lens, the wave vector can be written as follows:

$$\overrightarrow{K_1^e} = \left\{\frac{\sin\alpha}{n_e} + \eta_0^{"}\frac{\text{ltg}\theta+\text{decos}\varphi_e}{R}; \eta_0^{"}\frac{\text{decos}\varphi_e}{R}; \sqrt{1-\frac{\sin^2\alpha}{n_e^2}} - \eta_0^{"}q_z^{|}\right\} \quad (21)$$

If the unit vectors of optical axes are set as:
$\overrightarrow{a_1} = \{0, 0, 1\}$; $\overrightarrow{a_2} = \{\cos\varphi_0; \sin\varphi_0; 0\}$

then from the expressions (7), (9), (13) and (14) we will get respectively:

$$d_{00} = \frac{\left(1-\frac{\sin^2\alpha}{n_0^2}\right)\cos^2\varphi_0}{1-\frac{\sin^2\alpha}{n_0^2}\cos\varphi_0} \quad (22)$$

$$d_{0e} = \frac{\sin^2\varphi_0}{1-\frac{\sin^2\alpha}{n_0^2}\cos^2\varphi_0} \quad (23)$$

$$d_{ee} = \frac{\left(1-\frac{\sin^2\alpha}{n_0^2}\right)\cos^2\varphi_0}{1-\frac{\sin^2\alpha}{n_e^2}\cos^2\varphi_0} \quad (24)$$

$$d_{e0} = \frac{\sin^2\varphi_0}{1-\frac{\sin^2\alpha}{n_e^2}\cos^2\varphi_0} \quad (25)$$

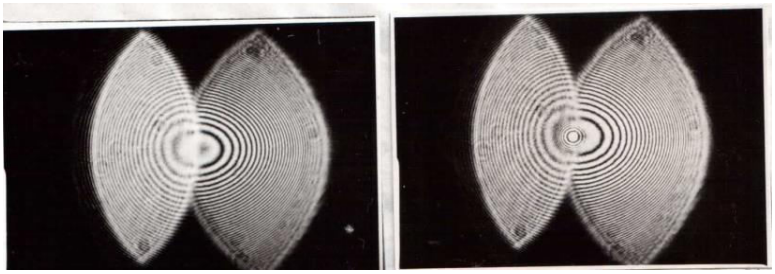

1 2

a.- oo, oe , ee и eo – beams,
1- without an analyzer, 2- with an analyzer

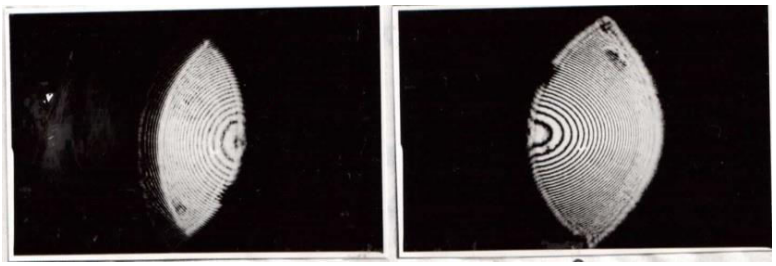

1 2

b. 1 - oo, eo - beams of the same polarization are distinguished by an analyzer
2 - ee, oe - beams of the same polarization are distinguished by an analyzer

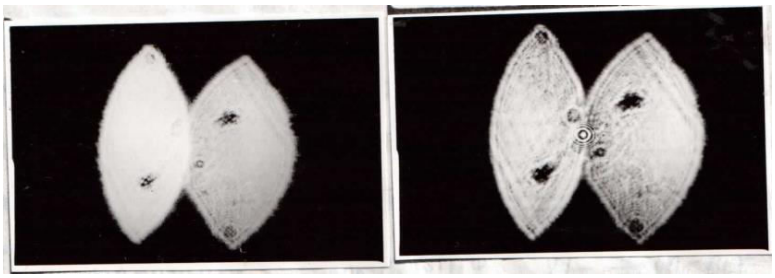

1 2

c.- oo , ee- orthogonally polarized beams,
1- without an analyzer, 2- with an analyzer.

Figure-3. Interference registries generated by the CCOS-1 in the collimated laser beam falling on the input face at an arbitrary angle / $\alpha=30^0$/ / "without an analyzer" mode of interference /.

Thus, as can be seen from the expressions (22), (23), (24) and (25), at $\varphi_0 = \frac{\pi}{4}$ there are four waves at the output of the CCOS-1 with approximately the same intensity (Figure 1a). At $\varphi_0 = 0$ we have $d_{00} = d_{ee} = 1$ and regardless of the incidence angle of the radiation on the input face of the CCOS-1, the basic waves at the output of the BL-1 will be (oo) and (ee) waves (Figure 1b).

Let us consider the interference properties of the lens of the CCOS-2 type. Start with the simplest case of a collimated laser beam that is normally falling on the input face of the CCOS-2 at z=0 (Figure 4). At the output of the CCOS-2 there are formed two main (oe) and (eo) waves. Partial (oe) and (eo) beams entering the CCOS-1 at the points $M_0(d_0 \cos\varphi\,, d_0 \sin\varphi, 0)$ and $M_e(d_e \cos\varphi\,, d_e \sin\varphi, 0)$, respectively, at the output of the CCOS-1 have the wave vectors derived from (12) and (14) at $\varphi = \frac{\pi}{2}$:

$$\overrightarrow{K_3^{0e}} = \left\{\frac{d_0}{R}(n_0 - n_e)\cos\varphi;\ \frac{d_0}{R}(n_0 - n_e)\sin\varphi;\ \sqrt{1 - \frac{d_e^2}{R^2}(n_0 - n_e)^2}\right\} \quad (26)$$

and

$$\overrightarrow{K_3^{eo}} = \left\{\frac{d_e}{R}(n_e - n_o)\cos\varphi;\ \frac{d_e}{R}(n_e - n_o)\sin\varphi;\ \sqrt{1 - \frac{d_e^2}{R^2}(n_e - n_o)^2}\right\} \quad (27)$$

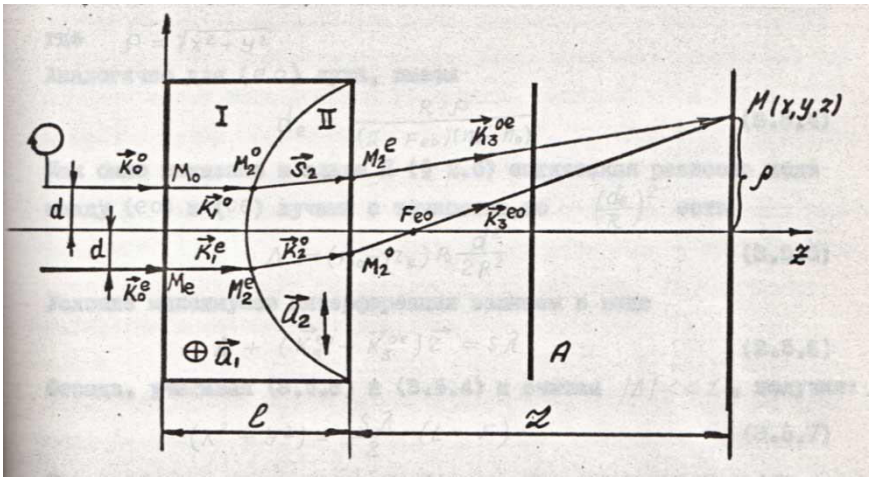

Figure-4. A scheme of polarized beams transmission through the CCOS-2 in the collimated laser beam

The formula (26) and (27) show that (oe) beams at the output of the CCOS-2 provide a divergent beam, and (eo) - convergent. Suppose the partial (oe) and (eo) beams intersect at the point M (x, y, z) at the screen (Figure-2). A direct calculation of transmission of the (oe) beam within the accuracy of $\left(\frac{d_0}{R}\right)^2$ with regard to (26) allows to find its input parameter:

$$d_0 = \frac{R\rho}{(z-F_{oe})(n_0-n_e)}\ , \qquad (28)$$

where $\rho = \sqrt{x^2+y^2}$
Similarly, for the (eo) beam, we have

$$d_e = \frac{R\rho}{(z-F_{eo})(n_e-n_o)} \qquad (29)$$

As shown previously, the optical transmission difference between (eo) and (oe) beams within the accuracy of $\left(\frac{d_0}{R}\right)^2$ is follows:

$$\Delta = (n_0 - n_e)R\frac{d^2}{2R^2} \qquad (30)$$

The condition of interference maxima can be written as follows:

$$\Delta + \left(\overrightarrow{K_3^{eo}} - \overrightarrow{K_3^{oe}}\right)\vec{r} = S\lambda \qquad (31)$$

Hence, taking into account (28) and (29) and supposing that $|\Delta| << 1$, we get:

$$(x^2+y^2) = \frac{S\lambda}{2}(L-F) \qquad (32)$$

Thus, the collimated beam when transmitting through the CCOS-2 provides an interference pattern in the form of rings with radii:

$$R_S = \sqrt{\frac{S\lambda}{2}(L-F)} \qquad (S=1, 2, 3) \qquad (33)$$

at the distance between the adjacent rings (for S>> 1):

$$\Delta R = \frac{\lambda(L-F)}{4R_S} \qquad (34)$$

This distance is proportional to the wavelength and inversely proportional to the radius of the S-th ring.

When the CCOS-2 is illuminated with the divergent laser beam, the interference pattern is getting complicated, and if the beams are moved in the transverse direction, i.e. in the xy plane, then the interference pattern is essentially dependent on the direction of transverse movement of the laser beam. All changes can be described by the method mentioned above. We will consider the "basic" (oe) and (eo) - beams.

a) the oe - wave

Suppose the axis of the divergent incident beam is determined by the equations x=0; y=d_0 (Figure 5). Let us represent the field in the divergent beam in the form of a system of divergent plane waves defined by the unit wave vector:

$$\overrightarrow{K_0} = \{\alpha\cos\varphi;\ \alpha\sin\varphi;\ 1\} \qquad (35)$$

A consistent consideration of the refraction of waves (35) at the interface in the CCOS-1 gives the following equations for the unit wave and radial vectors in the fields I and II of the CCOS-2 and at the output of the CCOS-2:

$$\overrightarrow{K_1^0} = \left\{\frac{\alpha\cos\varphi}{n_0};\ \frac{\alpha\sin\varphi}{n_0};\ 1\right\}$$

$$\overrightarrow{K_2^e} = \left\{\left[1+\frac{\delta}{2}\left(\frac{z_0}{R}n_e+\frac{\sigma}{R}\right)\right]\frac{\alpha\cos\varphi}{n_0}-\frac{\delta}{2}\frac{d_0}{R}\cos\varphi_0;\ \left[1+\frac{\delta}{2}\left(\frac{z_0}{R}n_e+\frac{\sigma}{R}\right)\right]\frac{\alpha\sin\varphi}{n_0}-\ -\frac{\delta}{2}\frac{d_0}{R}\sin\varphi_0;\ 1\right\} \quad (36)$$

$$\overrightarrow{K_3^e} = \left\{\left[1+\frac{\delta}{2}\left(\frac{z_0}{R}n_e+\frac{\sigma}{R}-1\right)\right]\alpha\cos\varphi-\frac{\delta}{2}\frac{d_0}{R}n_e\cos\varphi_0;\ \left[1+\frac{\delta}{2}\left(\frac{z_0}{R}n_e+\frac{\sigma}{R}-\ -1\right)\right]\alpha\sin\varphi\ -\frac{\delta}{2}\frac{d_0}{R}n_e\sin\varphi_0;\ 1\right\}$$

$$\overrightarrow{S_2} = \left\{\left[1+\frac{\delta}{2}\left(\frac{z_0}{R}n_e+\frac{\sigma}{R}\right)\right]\frac{\alpha\cos\varphi}{n_0}-\frac{\delta}{2}\frac{d_0}{R}\cos\varphi_0;\ \left[1+\frac{\delta}{2}\left(\frac{z_0}{R}n_e+\frac{\sigma}{R}\right)\right]\frac{\alpha\sin\varphi}{n_0}-\ -\frac{\delta}{2}\frac{d_0}{R}\sin\varphi_0;\ 1\right\}$$

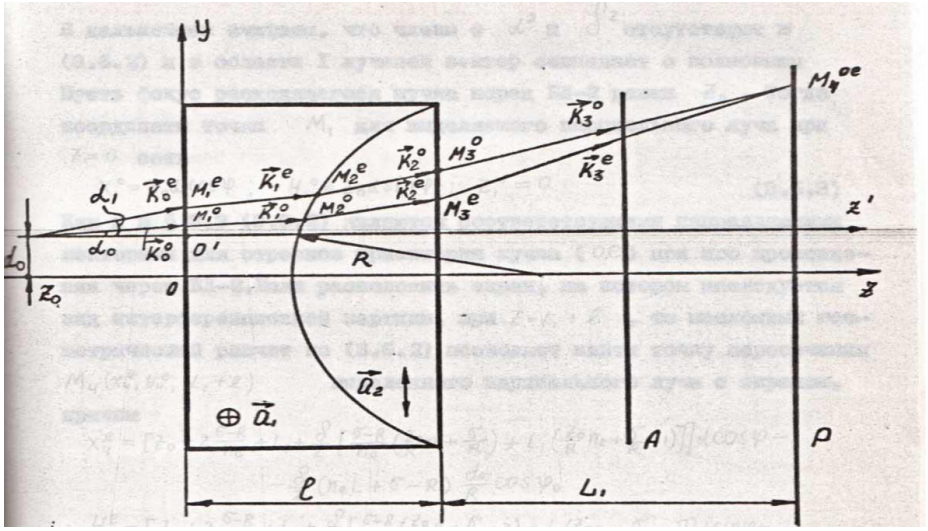

Figure-5. a. A scheme of polarized beams transmission through the CCOS-2 in the divergent laser beam displaced in the transverse / in the xy plane / direction.

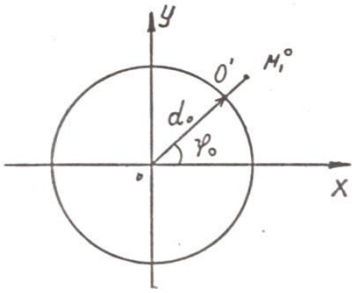

b. Location of points and parameters in the XY plane.

Then suppose that there are no members with α^2 и δ^2 andα^2 и δ^2, and in (2) in the field I the radial vector coincides with the wave one. Suppose that the focus of the divergent beam over the CCOS-2 is z_0. Then the coordinates of M_1 points for the selected partial beam at z=0 are

$$x_1^0 = z_0\alpha\cos\varphi;\ y_1^0 = z_0\alpha\sin\varphi;\ z_1^0 = 0 \quad (37)$$

As in (36), they are the corresponding directing vectors for the segments of the beam's trajectory (oe) as it passes through the CCOS-2. If we place the screen on which the form of the interference pattern is studied at $Z=L_1+l$, then the simple geometric calculation by (36) allows to find the intersection point $M_4(x_4^0, y_4^0, L_1+l)$ of the selected partial beam with the screen, wherein:

$$x_4^e = \left[z_0+2\frac{\sigma-R}{n_0}+L_1+\frac{\delta}{2}\left[\frac{\sigma-R}{n_0}\left(\frac{z_0}{R}n_0+\frac{\sigma}{R}\right)+L_1\left(\frac{z_0}{R}n_0+\frac{\sigma}{R}-1\right)\right]\right]\alpha\cos\varphi-\ -\frac{\delta}{2}(n_eL+\sigma-R)\frac{d_0}{R}\cos\varphi_0$$

$$y_4^e = \left[z_0+2\frac{\sigma-R}{n_0}+L_1+\frac{\delta}{2}\left[\frac{\sigma-R}{n_0}\left(\frac{z_0}{R}n_0+\frac{\sigma}{R}+2\right)+L_1\left(\frac{z_0}{R}n_0+\frac{\sigma}{R}-1\right)\right]\right]\alpha\sin\varphi-\ -\frac{\delta}{2}(n_eL_1+\sigma-R)\frac{d_0}{R}\sin\varphi_0 \quad (38)$$

$$y_4^e = L_1+2(\sigma-R);,$$

where $\sigma-$ is the distance from the origin of coordinates to the center of the spherical surface.

b) the eo - wave.

Suppose that at the input of the CCOS-2 for the (eo) beam the partial wave vector forms the angles α_1, и φ_1, and α_1, и φ_1, that differ from α и φ and

α и φ for the (oe) beam. For the (eo) wave the radial and wave vectors are of the form

$$\overrightarrow{S_1} = \left\{\frac{\alpha_1\cos\varphi_1}{n_e}(1+\delta);\ \frac{\alpha\cos\varphi_1}{n_e};1\right\}$$
$$\overrightarrow{K_1^e} = \left\{\frac{\alpha_1\cos\varphi_1}{n_e};\ \frac{\alpha_1\cos\varphi_1}{n_e};1\right\} \quad (39)$$

$$\overrightarrow{K_2^o} = \left\{\left[1-\frac{\delta}{2}\left(\frac{z_o}{R}n_e+\frac{\sigma}{R}\right)\right]\frac{\alpha_1\cos\varphi_1}{n_e}+\frac{\delta}{2}\frac{d_0}{R}\cos\varphi_0;\ \left[1-\frac{\delta}{2}\left(\frac{z_0}{R}n_e+\frac{\sigma}{R}\right)\right]\frac{\alpha_1\sin\varphi_1}{n_e}+\ +\frac{\delta}{2}\frac{d_0}{R}\sin\varphi_0;1\right\}$$
$$\overrightarrow{K_3^o} = \left\{\left[1-\frac{\delta}{2}\left(\frac{z_o}{R}n_e+\frac{\sigma}{R}-1\right)\right]\alpha_1\cos\varphi_1+\frac{\delta}{2}\frac{d_0}{R}n_e\cos\varphi_0;\ \left[1-\frac{\delta}{2}\left(\frac{z_0}{R}n_e+\frac{\sigma}{R}--1\right)\right]\alpha_1\sin\varphi_1+\frac{\delta}{2}\frac{d_0}{R}n_e\sin\varphi_0;1\right\}$$

The coordinates of the M_1^0 point of the input of the (eo) beam are as follows:

$$x_1^e = z_0\alpha_1\cos\varphi;\ y_1^e = z_0\alpha_1\sin\varphi;\ z_1^e = 0 \quad (40)$$

As for the (oe) - beam by (39) and (40) after the solution of the corresponding geometric problem we find the coordinates of the intersection points of the partial beam with the screen:

$$x_4^0 = \left[z_0+2\frac{\sigma-R}{n_e}+L_1-\frac{\delta}{2}\left[\frac{\sigma-R}{n_e}\left(\frac{z_0}{R}n_e+\frac{\sigma}{R}-2\right)+L_1\left(\frac{z_0}{R}n_e+\frac{\sigma}{R}-1\right)\right]\right]\alpha_1\cos\varphi_1+\ +\frac{\delta}{2}(n_eL_1+\sigma-R)\frac{d_0}{R}\cos\varphi_0$$
$$y_4^0 = \left[z_0+2\frac{\sigma-R}{n_e}+L_1-\frac{\delta}{2}\left[\frac{\sigma-R}{n_e}\left(\frac{z_0}{R}n_e+\frac{\sigma}{R}-2\right)+L_1\left(\frac{z_0}{R}n_e+\frac{\sigma}{R}-1\right)\right]\right]\alpha_1\sin\varphi_1+\ +\frac{\delta}{2}(n_eL_1+\sigma-R)\frac{d_0}{R}\sin\varphi_0 \quad (41)$$
$$z_4^0 = 2(\sigma-R)+L_1;$$

The condition for the interference maximum is also written in the following form:

$$\Delta+\left(\overrightarrow{K_3^{eo}}-\overrightarrow{K_3^{oe}}\right)\vec{r} = S\lambda \quad (S=0;\ \pm1;\ \pm2;)\ (3.6.8), \quad (42)$$

where $\lambda-$ is the wavelength; $\vec{r}-$ the radius vector of the observation point;

$\Delta = \delta\frac{d_0}{R}\frac{\sigma-R}{n_e}(\alpha_1+\alpha)\cos(\varphi_0-\varphi_1)$ - the path difference of the (eo) and (oe) beams at the output of the CCOS-2.

The connection between the input angles α, φ, α_1, φ_1, and the coordinates of the observation point can be obtained from the condition that the points M_4^0 и M_4^e and M_4^0 и M_4^e are identical. Using (38) and (42), we obtain the condition for the maxima:

$$x^2\left[z_0^2+\frac{l}{n_0}z_0+\frac{lR}{2n_e^2}+\frac{l^2}{4n_0^2}\right]+y^2\left[z_0^2+\frac{l}{n_e}z_0-\frac{lR}{2n_e^2}+\frac{l^2}{4n_0^2}\right]-$$
$$\frac{d_0}{R}\left[z_0^2+\ +z_0\frac{l}{2n_e^2}(3n_e+1)+\frac{l^2}{2n_e^2}\frac{n_e+1}{n_e}+L_1\left(z_0+\frac{l}{2n_e}+\frac{l}{2n_e^2}\right)\right](x\cos\varphi_0+\ y\sin\varphi_0) = =\ S\lambda\frac{R}{n_e\delta}(L+L_1)^2 \quad (43)$$

where $L=z_0+2\frac{\sigma-R}{n_e}$

If we assume that the observation plane (p) is located close to the output face of the CCOS-2, i.e. L_1 is very small, then from (43) we have:

$$x^2\left[z_0^2+\frac{l}{n_0}z_0+\frac{lR}{2n_e^2}+\frac{l^2}{4n_0^2}\right]+y^2\left[z_0^2+\frac{l}{n_e}z_0-\frac{lR}{2n_e^2}+\right.$$
$$\left.\frac{l^2}{4n_0^2}\right]-\frac{d_0}{R}\left[z_0^2++z_0\frac{l}{2n_e^2}(3n_e+1)+\frac{l^2}{2n_e^2}\frac{n_e+1}{n_e}\right](x\cos\varphi_0+$$
$$y\sin\varphi_0) = S\lambda\frac{R}{n_e\delta}(z_0n_e+l)^2 \quad (44)$$

For the parameters used in the experiments with the CCOS-2

$$(l=7.4\text{мм},\ R=50.2\text{мм};\ n_e=1.49,\lambda=0.6328\text{мкм},\delta=0,2)$$
из (44)

we get the following equation of the second order curve:

$$x^2(z_0^2+5z_0+90)+y^2(z_0^2+5z_0-78)-\frac{d_0}{R}(x\cos\varphi_0+y\sin\varphi_0)(z_0^2+$$
$$+9.12z_0+20.6) = 5.5*10^{-2}\ (1.49z_0+7.4)^2 \quad (45)$$

The shape of this curve is shown in Figures 6 and 7.

If $d_0=0$, then from (43) we obtain

$$\left(z_0^2+\frac{l}{n_0}z_0+\frac{lR}{2n_e^2}+\frac{l^2}{4n_0^2}\right)x^2+\left(z_0^2+\frac{l}{n_e}z_0-\frac{lR}{2n_e^2}+\right.$$
$$\left.\frac{l^2}{4n_0^2}\right)y^2 = \frac{R\lambda S}{\delta n_e^3}\ (z_0n_e+l+\ +ln_e)^2 \quad (46)$$

or

$$(z_0^2+5z_0+90)x^2+(z_0^2+5z_0-78)y^2 = 5.5*$$
$$10^{-2}\ (1.49(d_0+l)+7.4)^2 \quad (47)$$

The shape of this curve is determined by the coefficients in (47) (Figure-6). In the range of 6, $7>z_0>-11.7$ mm the interference pattern is shaped in the form of non-equilateral hyperboles that approach the non-equilateral hyperboles at $-3\leq z_0\leq-2$мм mm. For the values $6,7\geq z_0\geq-11,7$мм mm the hyperboles are transformed into ellipses. For the values $z_0>6.7$мм mm and $z_0<-11.7$мм mm the ellipses are getting close to the circles. The expression (47) gives a qualitative correspondence of theory with experiment.

If we make a calculation within the accuracy of α^3, then the path difference will be as follows:

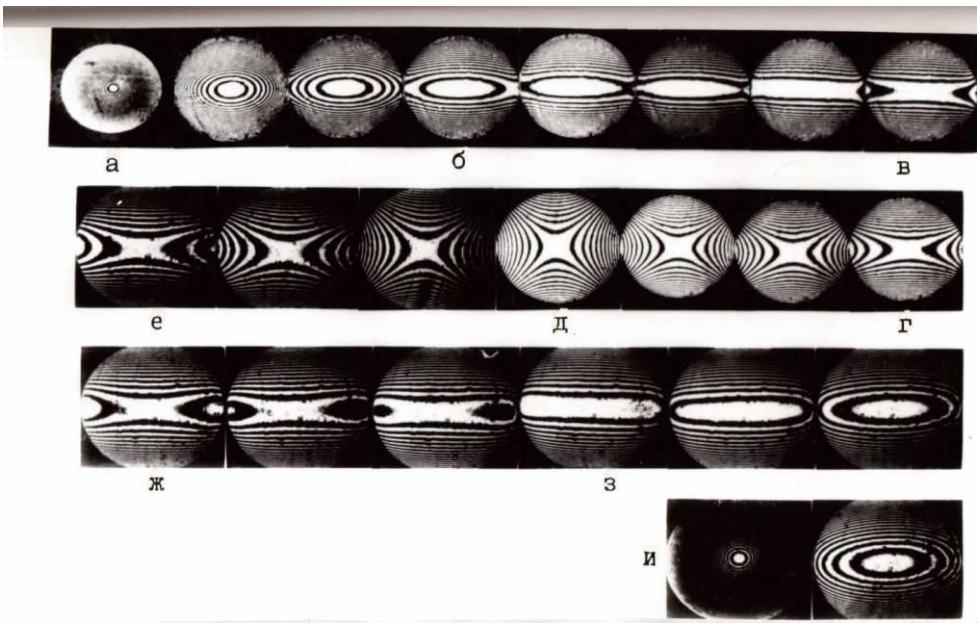

Figure-6. Interference patterns generated by the CCOS-2 with the longitudinal displacement of Δz / along the z axis / of the focused laser beam at the input. Pictures /а/-/и/ are for $\Delta z = +22, +12, +11, +10, +0, -5, -5.5, -6.5, -18$мм mm, respectively. $\Delta z = 0$ corresponds to the front face of the CCOS-2. /$-\Delta z$ / corresponds to the displacement of the focused laser beam to the front face of the CCOS-2.

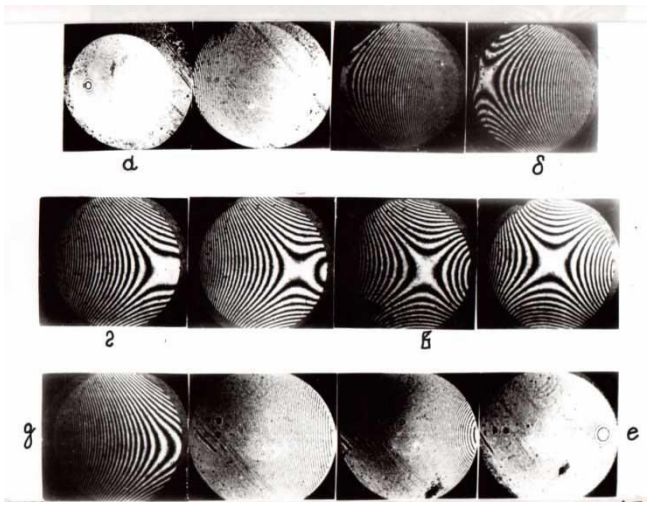

Figure-7. Interference patterns generated by the CCOS-2 with the displacement of Δz / of the z axis / of the focused laser beam displaced at a distance d=4 mm from the center of the CCOS-2 in the XY plane. Displacement occurs along the x-axis / at $\varphi_0 = 0$/. Pictures /а/-/и/ are for $\Delta z = 30, 3, 0, -3.5, -3, -25$мм mm, respectively. $\Delta z = 0$ corresponds to the front face of the CCOS-2. /$-\Delta z$ / corresponds to the displacement of the focused laser beam to the front face of the CCOS-2.

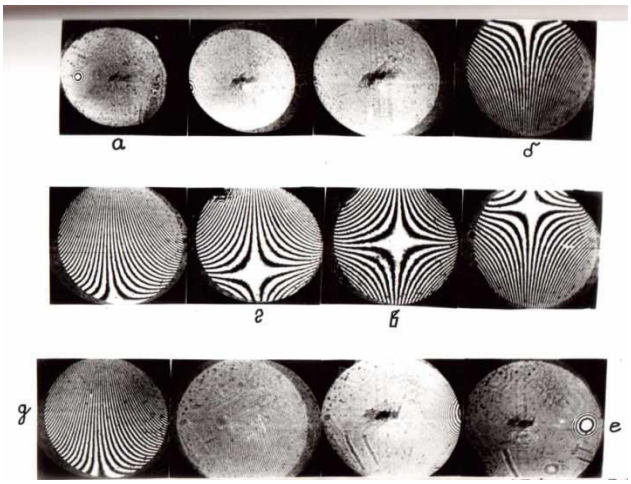

Figure-8. Interference patterns generated by the CCOS-2 with the displacement of Δz / of the z axis / of the focused laser beam displaced at a distance d=4 mm from the center of the CCOS-2 in the XY plane. Displacement occurs in the direction of the composing angle 45^0 with the axes X and Y / $\varphi_0 = 45^0$/. Pictures /а/-/и/ are for $\Delta z = 30, 5, 1, 5, 0, -4, -25$мм mm, respectively. $\Delta z = 0$ corresponds to the front face of the CCOS-2. /$-\Delta z$ / corresponds to the displacement of the focused laser beam to the front face of the CCOS-2.

between the (o) and (e) waves at the output of the CCOS-2 there is:

$$\Delta = \frac{l}{4}\frac{z_0}{R}\frac{\delta}{n_e}(\alpha^2 + \alpha_1^2) \quad (48)$$

Then the equation of the geometric place of points for the maxima of the interference pattern is written in the following form:

$$\left[z_0^2 + z_0\left(\frac{l}{n_e} + l - 2n_e^2\right) + \frac{eR}{2n_e^2} + \frac{l^2}{4n_e^2}\right]x^2 + \left[z_0^2 + z_0\left(\frac{l}{4} + l - 2n_e^2\right) - \frac{lR}{2n_e^2} + + \frac{l^2}{4n_e^2}\right]y^2 = \frac{RS\lambda}{\delta n_e^3}[(z_0 + l)n_e + l] \quad (49)$$

One of the well-known materials for the construction of the CCOS is an Iceland spar ($CaCO_3$), that has a high value of $\Delta n = n_0 - n_e = 0.17$. The dispersion of the Iceland spar was presented in Figure 9, for λ = 0,4 + 2,3 μm. In the visible field of the spectrum (λ = 0,4 + 0,7 μm) the change of the refraction index $CaCO_3$ for the o-beam is $\Delta n_0 = 0.032$, and for the e- beam is $\Delta n_0 = 0{,}016$. As seen from the dispersion curve of the Iceland spar, the values of Δn increase in the ultraviolet field of the spectrum and in the infrared field - decrease, remaining almost constant in the visible field. These small changes in the refraction indices of the Iceland spar, depending on the wavelength, give a significant effect of the change of focal distances of the CCOS.

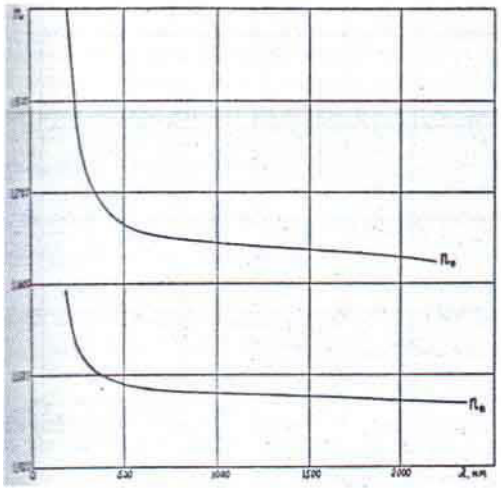

Кривая дисперсии исландского шпата ($CaCO_3$)

Figure-9. The dispersion curve of the Iceland spar ($CaCO_3$).

The experiment was conducted to measure the changes of the focal length of the CCOS, depending on the wavelength of radiation. Two waves were used: λ = 0, 6328 μm and λ = 1,15μm of the coherent radiation (LG-126).

The recording of the light intensity in focuses was carried out with the help of an infrared vidicon (LI-438) of PTU-32 installation. The spectra in the visible field were obtained from the source of "white" light using different polarization filters. In this case, the focal points of different wavelength were recorded by a microscope (OSM-2). Experimental results and theoretical calculation are presented in Figures 10 and 11.

As can be seen from Figures 10 and 11, with the decreasing of the wavelength, the focal distances (F_{ee} и F_{eo}) decrease, and the effect of increasing of the difference of focal distances $\Delta F = F_{eo} - F_{ee}$ is observed, and with the increasing of the wavelength there is an increase in the focal distances and a decrease in ΔF. The change of the difference of focal distances ΔF with the change of the wavelength of radiation becomes clear if to take into account that the trajectory of the e - beam in the field II of the CCOS-1 is given by the direction of the radial vector.

Changes of ΔF depending on the wavelength can be used for the selection of focal distances when using incoherent light sources.

It is necessary to note one more important feature of the CCOS-1 which consists in the ability to form an interference pattern using a "white" light source. When the CCOS-1 is illuminated by a convergent beam of "white" light, at the output of the CCOS-1 the interference pattern is formed in the shape of a light and dark cross with multicolored circles.

A variety of interference patterns in case of using "white" light is shown in Figure-12.

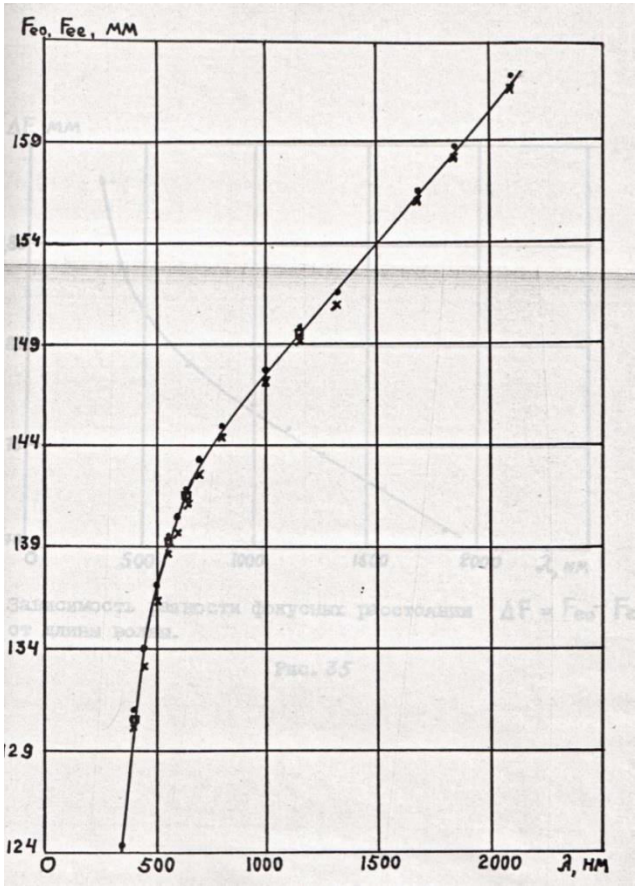

Figure-10. Dependence of the focal distance F_{oe} and F_{ee} on the wavelength. The calculated dependence of focal distances F_{oe} and F_{ee}, respectively, x, the experimental dependence of the focal distance F_{ee} = ■.

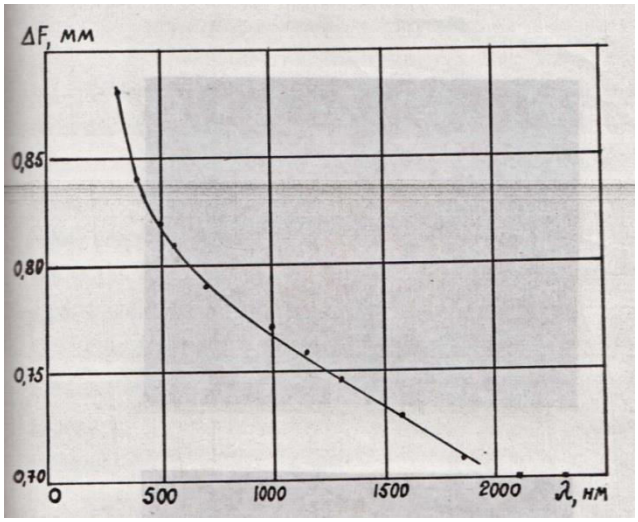

Figure-11. Dependence of the difference of focal distances $\Delta F=F_{oe}- F_{ee}$ on the wavelength.

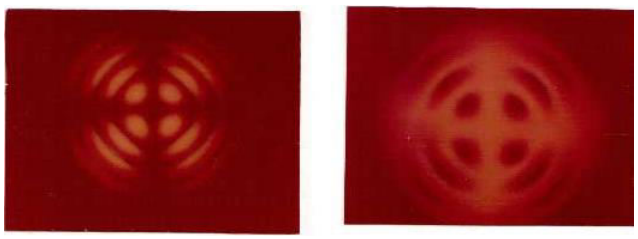

Figure-12. Interference patterns formed by the CCOS-I in the "white" light.

To get a full picture of the structure of the optical image, it is necessary to know the light distribution not only in the focal plane, but also near the focus, in the accurate restructuring of the system, having a large depth of focus. The exact definition of the location of the focal plane of the system plays an important role in holography.

The diffraction patterns of the optical field near the focuses and the dependence of the light intensity distribution in the focal plane on various primary aberrations are discussed by many researchers.

Here are some interesting observation results of the structure of the optical field near the focal plane of the CCOS-1 and CCOS-2.

A functional scheme of the installation is shown in Figure-13. The laser beam from the source 1, after its expansion by a collimator, including a micro-lens (2), a diaphragm (3) and a collimating lens (4), falls on the CCOS 5. The structure of the field near the focus of the CCOS is observed by a microscope OSM-2 of the sixth type, the accuracy of which by the internal scale of Archimedes spiral is 10 μm.

Figure-14 shows the results of observation of the optical field structure near the focuses Foe and Fe e of the CCOS-1. Section types of beams corresponding to different distances from the intended focus are presented. The sign "-" in Figure-14 means that the section of the beam is fixed to the intended focus from the direction of the CCOS-1.

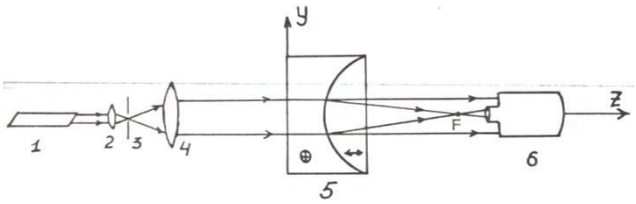

Figure-13. An installation scheme for monitoring the interference structure of the optical field in the CCOS focuses. Note. 1 - a gas laser, 2 - a microlens, 3 - a diaphragm, 4 - a collimating lens, 5 - CCOS-1, 6 - a microscope.

As can be seen from Figure 14, the distribution of light intensity in the focus area by the cross section of the beam is diverse. There are diffraction structures in the sections of the beam; the field near the focuses is "blurred", and the inexplicitly expressed focus is being formed.

When the CCOS-1 is rotated around the y axis (Figure-12), the field structures are changing. The peculiarities of change of the optical field structure near the focuses at the rotation of the CCOS-1 around the "y" axis at different angles are shown in Figure 15.

Variability of the distribution of light intensity in the focus area Fee at different values of $\Delta Z = 0$ -3; -5 mm is shown in Figures 16, 17 and 18. In this case, as compared to Figure-13, the CCOS-1 is rotated around the y-axis at 180°.

As noted in the experiment with the use of an ideal lens MIR-1, the diffraction structure of the field in the cross sections of the beam near the focus decreases. However, at a large turn angle of the lens MIR-1 around the y-axis, the structure of the field in the form of the caustic is observed.

For comparison with the obtained pictures, the optical field structure near the focus for a variety of lenses was studied. However, its mathematical description is a complex task; therefore, it is not considered in this article. Our purpose was to present some interesting experimental data of the characteristics of light intensity distribution near the focuses.

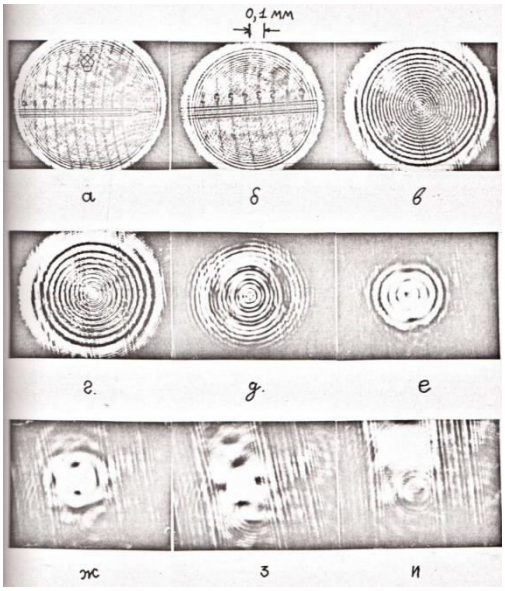

Figure-14. Section type of the laser beam focused with the help of the CCOS in different distance Δ Z from the focuses F_{oe} and F_{ee}. Pictures /a/ - /и/ are for Δ Z=-17, -14, -9, -7, -4, -2, -1, 0, +1 mm, respectively. The value of one large division of the ocular-micrometer is 0.1 mm. Δ Z=0 corresponds to the conditional focus of the CCOS. / - Δ Z / corresponds to the retraction of the microscope from the CCOS, i.e. in the course of the laser beam up to the conditional focus.

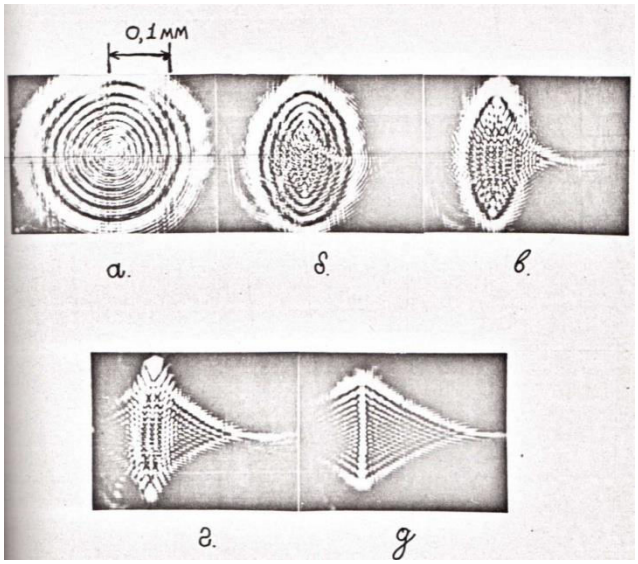

Figure-15. The interference field structure in the focal area of the CCOS-1 \for the focuses F_{oe} and F_{ee} at Δ Z=-5mm / in the laser radiation / λ=0,6328 μm /. Pictures /a/ - /д/ show the individual stages of observation of the caustic along the axis when the CCOS is rotated around the y-axis at an angle $\varphi=0^0,\ 5^0,\ 10^0, 12^0$, respectively. The pattern scale: the distance between the spiral lines of the ocular-micrometer is equal to 0.1 mm.

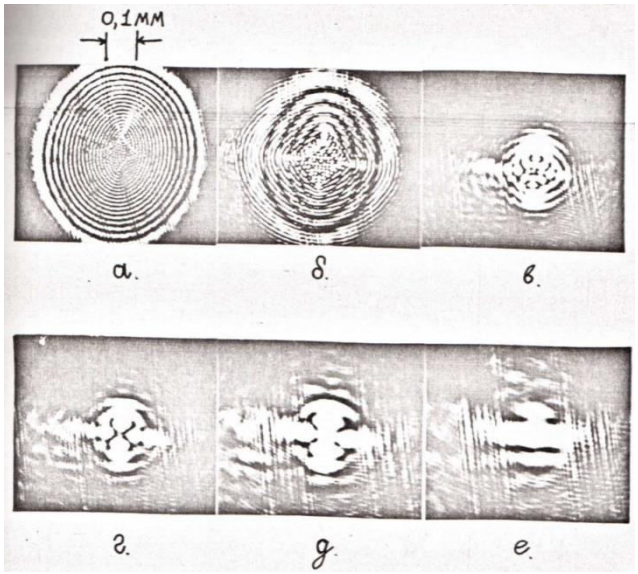

Figure-16. Section type of the laser beam / λ = 0, 6328 μm / focused with the help of the CCOS-1, depending on the distance of Z from the focus F_{ee}. Pictures /a/ - /e/ are for Δ Z= -11, -6, -5, -0, 5, 0, +1,5 mm, respectively. Photos are obtained when the CCOS-1 is turned at 1800 around the axis, as compared with Figure 13. Astigmatism can be noticed, as compared with Figure-14.

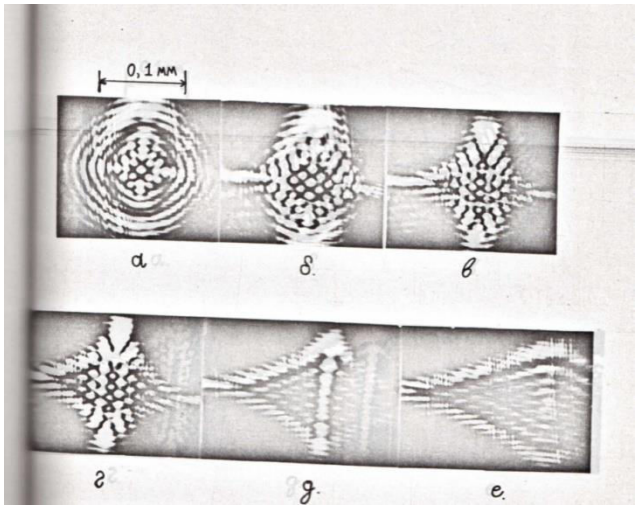

Figure-17. The interference field structure in the focal area F_{ee}at Δ Z= -3 mm. Pictures /a/ - /e/ show the individual stages of observation of the caustic along the Z-axis when the CCOS-1 is rotated around the y-axis at an angle $\varphi = 0^0,\ 7^0,\ 9^0, 11^0, 13^0, 16^0$, respectively. The pattern scale: the distance between the adjacent lines of the spiral of the ocular-micrometer is equal to 0.1 mm.

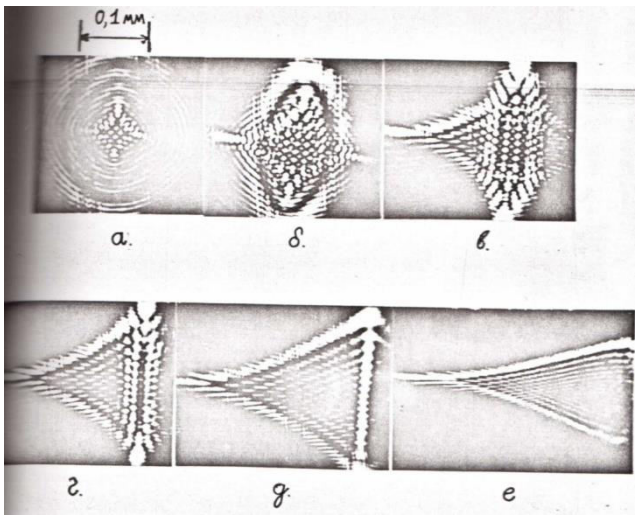

Figure-18. The interference field structure in the focal area F_{ee}at Δ Z= -5 mm. Pictures /a/ - /e/ show the individual stages of observation of the caustic along the Z-axis when the CCOS-1 is rotated around the Y-axis at an angle $\varphi = 0^0,\ 7^0,\ 11^0, 14^0, 17^0, 25^0$, respectively. The pattern scale: the distance between the adjacent lines of the spiral of the ocular-micrometer is equal to 0.1 mm.

4. `CONCLUSIONS

This paper studied the functioning of composite crystal optical systems of two types: CCOS-1 and CCOS-2 in the mode of interference of polarized beams.

The peculiarity of interference in the system of CCOS-1 type was theoretically described and experimentally justified. The interference of polarized beams was performed without analyzers when the optical axis was located in the input field of the CCOS-1 along the propagation direction of the laser beam.

There were obtained the expressions describing the dependence of the type of interference patterns formed in the CCOS-2 on the angle of radiation divergence, falling on the front face of the CCOS, on the longitudinal displacement (along the Z-axis) of the focused laser beam, and on the transverse displacement (in the xy plane) of the focused laser beam.

The interference structure of the optical field and its spatial transformation in the focal field during the laser irradiation of the CCOS was experimentally studied.

The experiments confirming the regularities of interference patterns allow recommending the use of the CCOS-1 and CCOS-2 in laser measuring devices.

The dispersion properties of the CCOS were considered. The focal lens distances of CCOS-1 and CCOS-2 types were measured depending on the length, and the calculations were made in the range of 0, 4 $<\lambda<$2,3 μm, which are in good agreement with each other.

The interference structure of the optical field in the focal area during the laser radiation of the CCOS was experimentally studied.

REFERENCES

[1] Bazykin. S.N. 2014. Information-measuring systems based on interferometers: monograph. Penza: PSU

[2] Demtreder. V. 2014. Modern laser spectroscopy. Moscow: Nauka.

[3] Hnatovsky.C. 2012. Polarization-dependent ablation of silicon using tightly focused fem to second laser vortex pulses, Optics letters. 37(2): 226-228.

[4] Wang. I. 2012. Development and prospect of near field optical measurements and characterizations, Optoelectron. 5(2): 171-181.

[5] Kotlyar.V.V. 2013. Analysis of the shape of a sub wavelength focal spot for the linear by polarized light, Applied optoelectronics. 52(3): 330-339.

[6] Khomina. S.N. 2012. Polarization converter for higher-order laser beams using a single binary diffractive optical element as beam splitter, Optics letters. 37(12): 2385-2387.

[7] Alferov. S.V. 2014. Experimental research of the focus of nonuniformly polarized beams generated by means of sector plates, Computer Optics. 38(1): 57-66.

[8] Venkatarrishnan. K. 2012. Generation of radically polarized beam for laser micromachining. Journal of Laser Micro/Nanoengineering. 7(3): 274-278.

[9] Golovashkin. D.L. 2012. Computer Design of Diffractive Optics. Cambridge: Wood head Publishing Limited.

[10] Khomina. S.N. 2014. Theoretical and experimental study of polarized changes in uniaxial crystals for obtaining cylindrical vector beams of higher orders. Computer Optics. 38(2): 171-180.

[11] Tarasevich.B.N. 2012. Fundamentals of infrared Fourier transform spectroscopy. Moscow: Nauchanya Musl.

[12] Porfiriev. L.F. Fundamentals of the theory of signal transformation in optoelectronic systems. Saint Petersburg, Lan.

[13] Yakushenkov. Y.G. 2013. Fundamentals of optoelectronic instrumentation. Moscow: Logos.